Supporting Information

One-Dimensional Ag NW@NiCo/NiCo(OH)$_2$ Core-shell Nanostructured Electrode for Flexible and Transparent Asymmetric Supercapacitor

Junyan Liu, Gengzhe Shen, Sirou Zhao, Xin He*, Chi Zhang*, Tinghui Jiang, Jiayi Jiang, Bohua Chen

School of Applied Physics and Materials, Wuyi University, Jiangmen 529020, Guangdong Province, P.R. China.

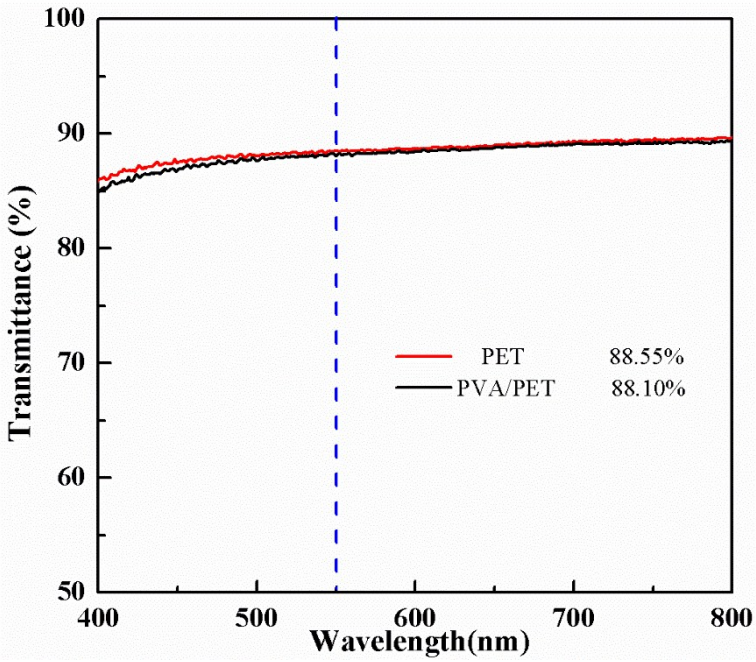

Fig. S1 Optical transmittance spectra of the blank PET before and after depositing PVA layer.

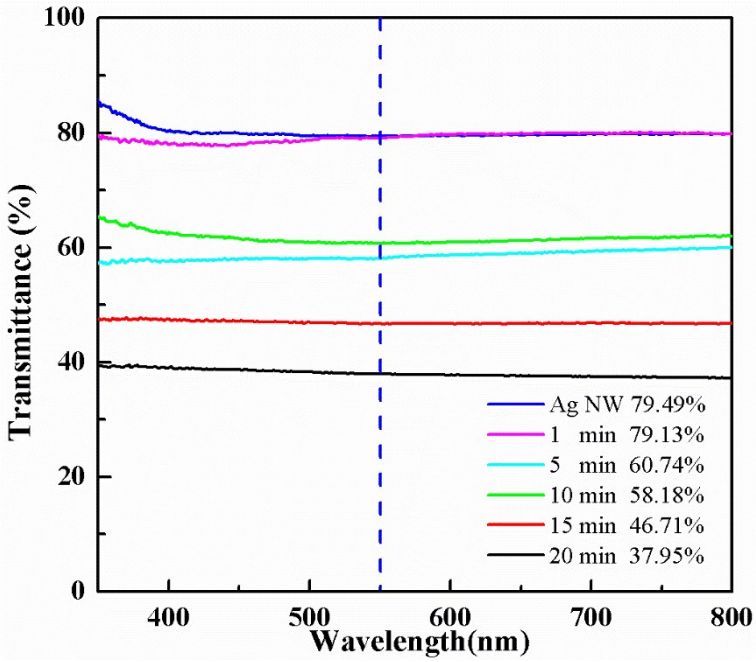

Fig. S2 Optical transmittance spectra of the Sample 2 deposited for 1, 5, 10, 15 and 20 min, respectively.

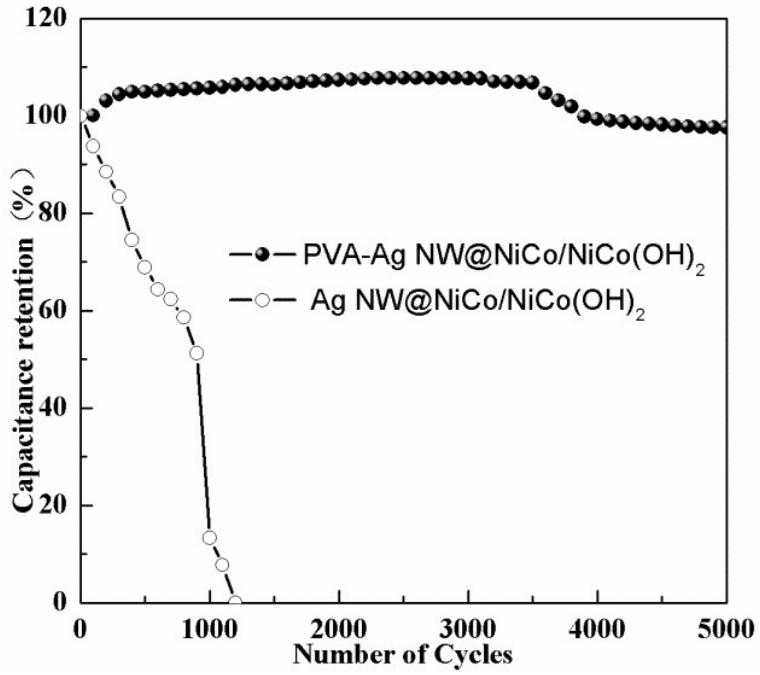

Fig. S3 Cycling performances of the Ag NW@NiCo/NiCo(OH)$_2$ and PVA-Ag NW@NiCo/NiCo(OH)$_2$ electrodes at a scan rate of 100 mV/s for 5000 cycles.

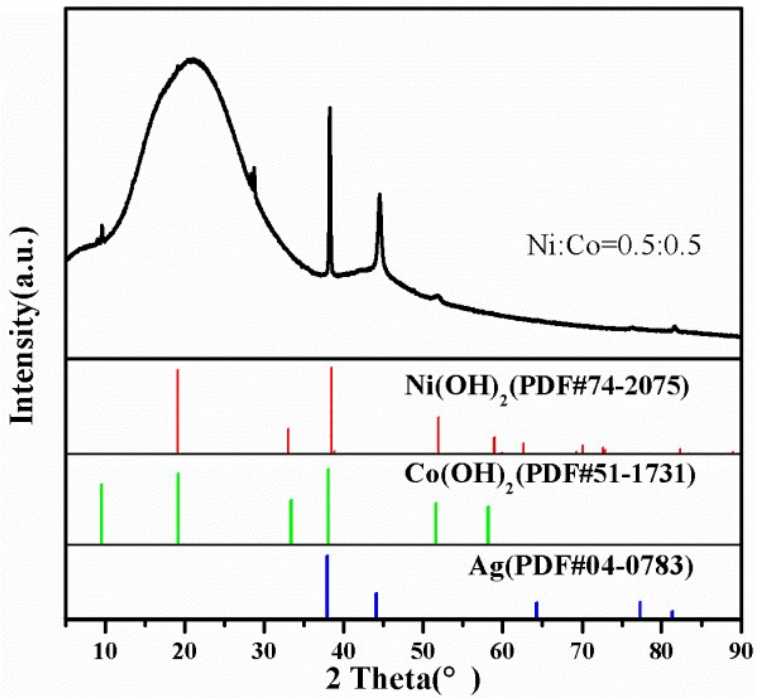

Fig. S4 XRD patterns of the Sample 3 with Ni to Co ratio of 0.5 : 0.5 after 5000 cycles.

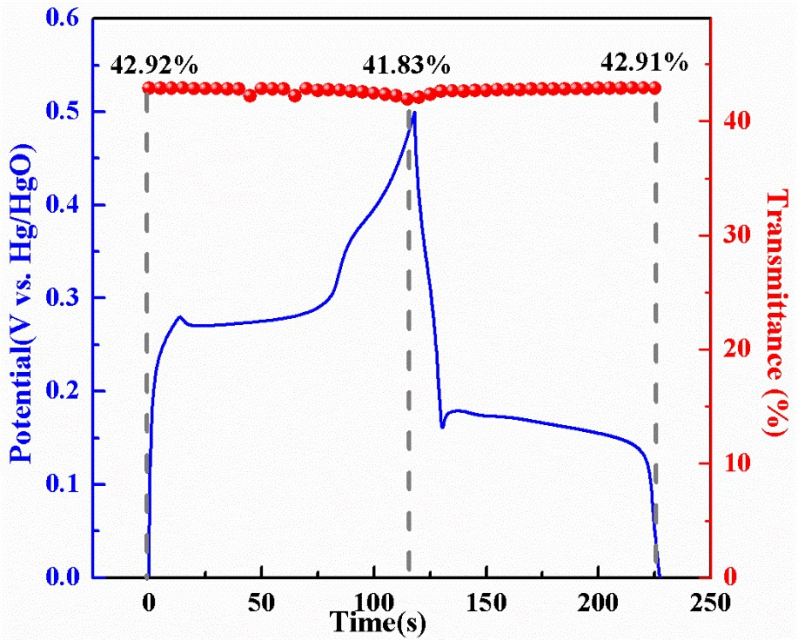

Fig. S5 Optical transmittance spectra of the Sample 2 during charging and discharging process.

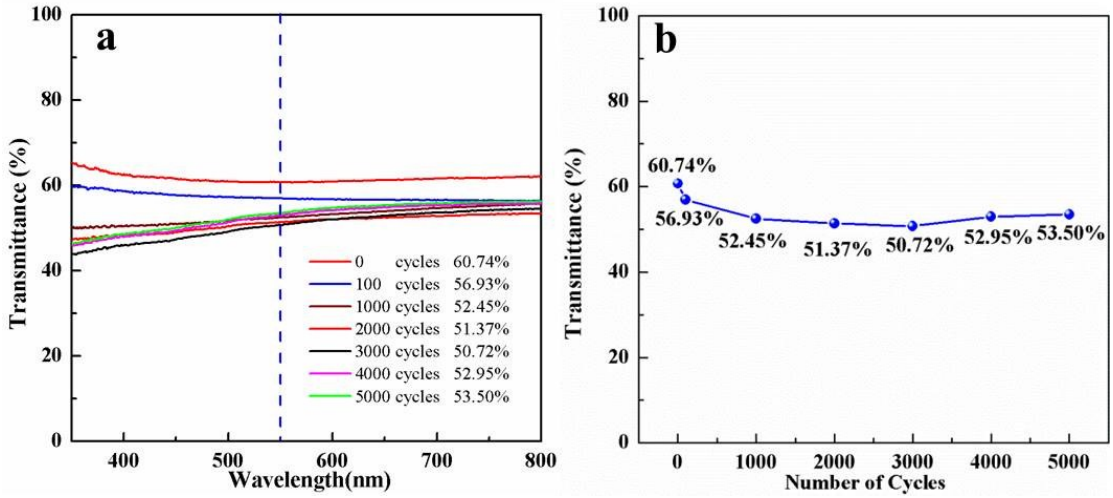

Fig. S6 (a) Optical transmittance spectra of the Sample 2 after 100, 1000, 2000, 3000, 4000 and 5000 charge-discharge cycles, respectively; (b) the transmittances at 550 nm as the function of the number of cycles.

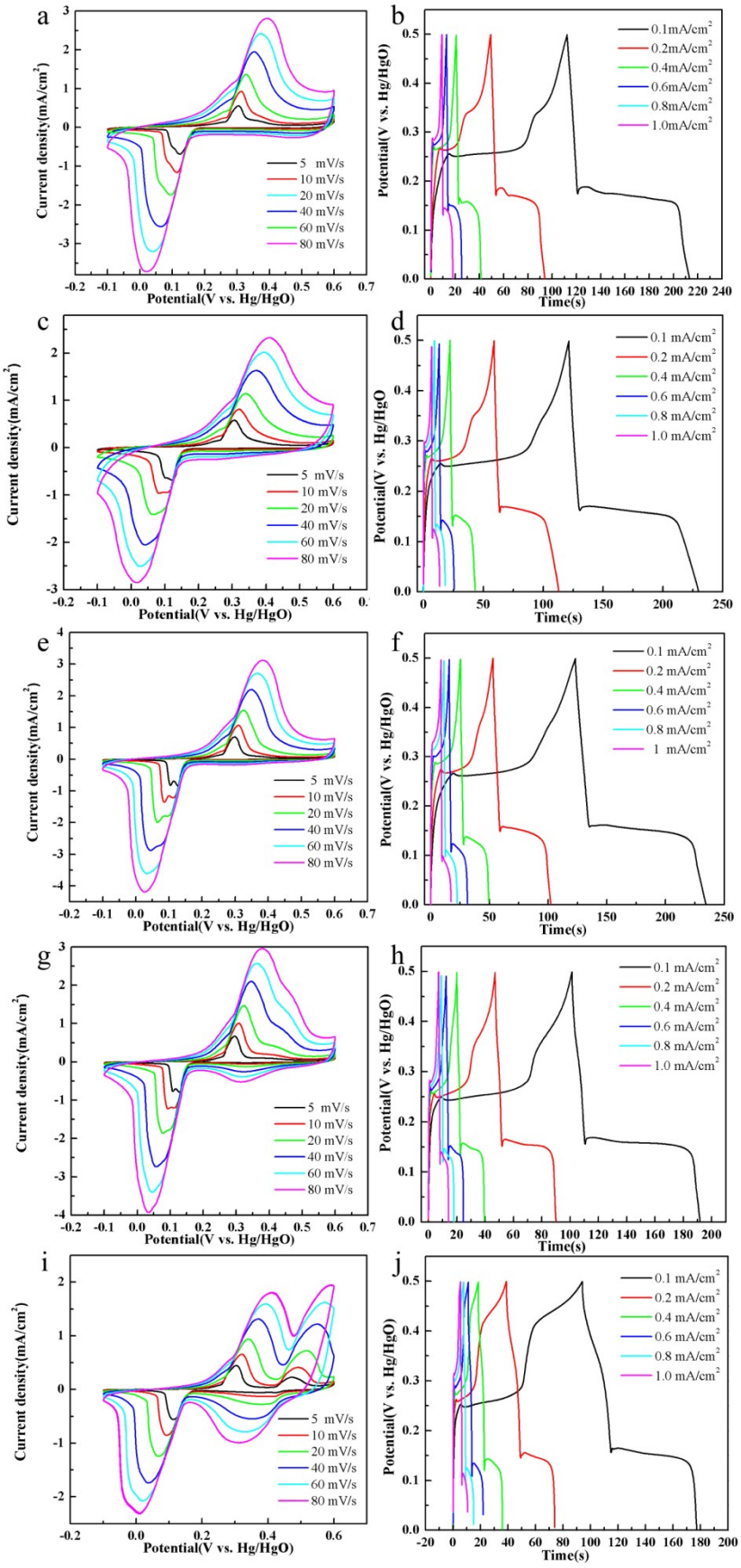

Fig. S7 CV curves of five samples at various scan rates (a, c, e, g and i). GCD curves of five samples collected at various current densities with (b, d, f, h and j).

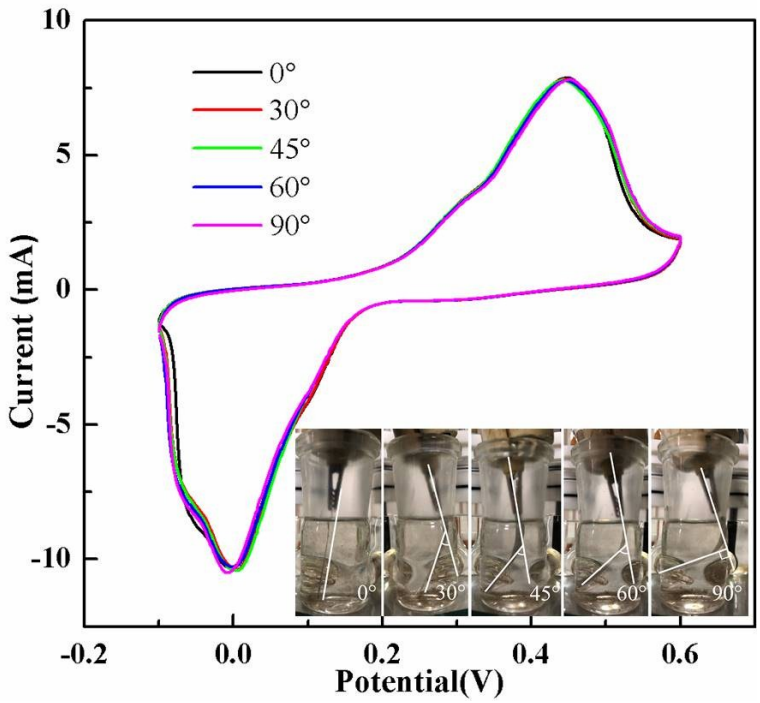

Fig. S8 CV curves of the Ag NW@NiCo/NiCo(OH)$_2$ electrode with the bending angles of 0, 30°, 60°and 90°; the inset image is the photographs of the corresponding bent states.

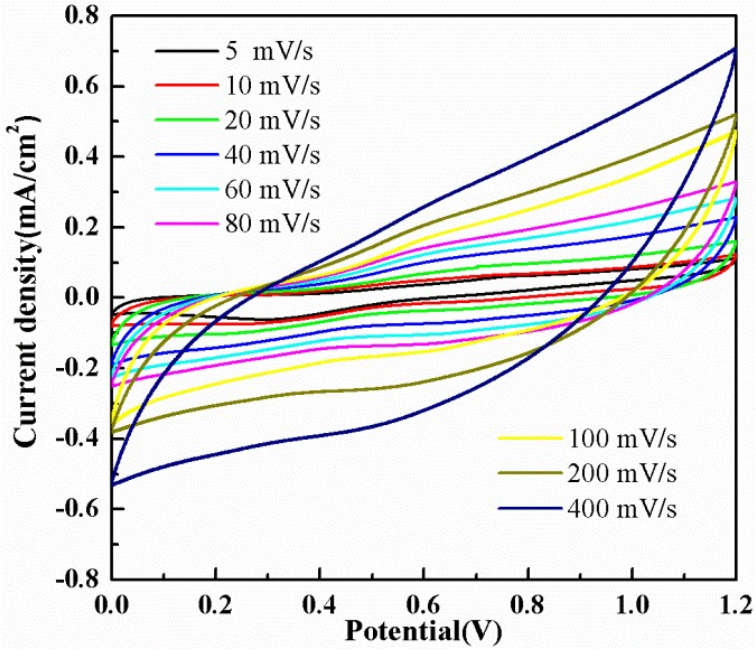

Fig. S9 CV curves of the asymmetric supercapacitor at various scan rates.

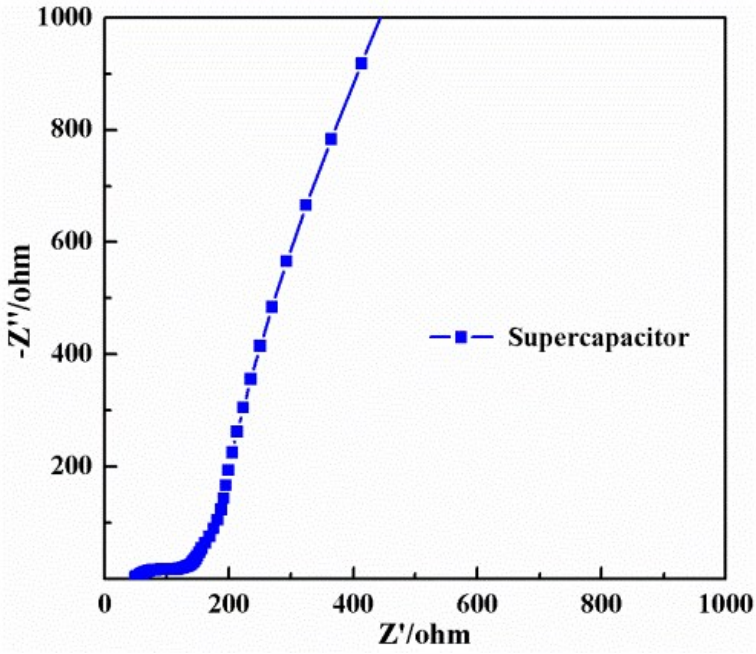

Fig. S10 Nyquist impedance spectrum of the asymmetric supercapacitor.

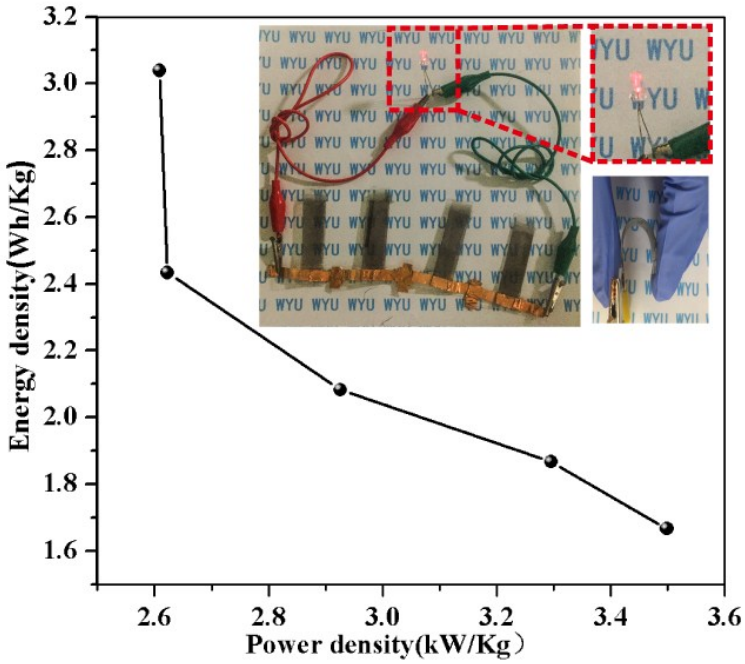

Fig. S11 Ragone plot of the supercapacitor; the inset is an LED driven by four devices connected in series.